View Article Online / Journal Homepage / Table of Contents for this issue

J. CHEM. SOC. FARADAY TRANS., 1990, 86(12), 2253–2261

Dilute Lamellar and L_3 Phases in the Binary Water–$C_{12}E_5$ System

Reinhard Strey and Reinhard Schomäcker
Max Planck Institut für Biophysikalische Chemie, Postfach 2841, D-3400 Göttingen, Federal Republic of Germany
Didier Roux, Frederic Nallet and Ulf Olsson*†
Centre de Recherche Paul-Pascal, Château Brivazac, F-33600 Pessac, France

Published on 01 January 1990. Downloaded by Max Planck Institut fuer on 11/01/2017 11:20:10.

The binary phase diagram of water–$C_{12}E_5$ has been studied with emphasis on the L_3 and dilute lamellar phases, which were found to swell to approximately 99.5 and 98.8 wt % of water, respectively, much further than has been reported previously. Focusing on these two phases, we have carried out static light and small-angle neutron scattering and electrical conductivity measurements. The repeat distance in the lamellar phase was found to exceed 3000 Å. A small, but significant deviation from ideal one-dimensional swelling was observed. This deviation may be explained in terms of flexibility of the bilayers that are flat only on average. Electrical conductivity and small-angle neutron scattering data from the isotropic L_3 phase are, over most of the stability range, consistent with a three-dimensional continuous bilayer structure. However, at large water contents an increase in the conductivity indicates a breakup of the structure into smaller fragments. Our results show that the simpler binary system exhibits the same characteristic features as the more complex multicomponent systems, involving brine, ionic surfactant and cosurfactant.

Surfactant systems show a rich variety of phase behaviour, which is related to the numerous ways in which space may be divided into polar and apolar regions for a given surface-to-volume ratio. A large number of liquid and liquid-crystalline phases, leading to very complex phase diagrams, have been observed.[1] Surfactants aggregate in solution to form monolayers of oriented molecules separating polar and apolar regions. Depending on the conditions, such monolayers may enclose a finite volume, as in micelles, or be continuous in one, two or three dimensions.[2] In certain cases, two oppositely oriented monolayers may join to form a bilayer separating two equivalent solvent domains.

A lot of interest has recently been focused on systems where the surfactant monolayer, or bilayer is flexible.[3] The rigidity of the surfactant film or membrane is characterized, by means of an elastic energy density,[4] in terms of a bending modulus, κ. The surfactant interface is flexible when κ is of the order of the thermal energy, k_BT; the amplitude of its thermal undulations then becomes comparable to typical structural length scales in the system. One particular consequence of high-amplitude thermal undulations is the long-range repulsive interaction between surfactant monolayers or bilayers, originating from the loss of configurational entropy when the layers are stacked.[5] This interaction has been proposed to account for the large swelling of certain lamellar phases in the absence of strong repulsive electrostatic interactions. Recent high-resolution X-ray[6,7] and dynamic light scattering[8,9] studies have established that this steric interaction indeed dominates in certain systems and yields values of κ of the order of k_BT. Systems, exhibiting flexible films or membranes, have been mostly encountered in complex quaternary (or quinary) ionic surfactant–cosurfactant–solvent mixtures, where the flexibility is induced by presence of cosurfactant (usually a short-chain alcohol).[10] General patterns in the phase behaviour[11,12] and physicochemical properties[13] have been shown to be common to the more complex quinary systems and the simpler ternary systems of water, oil and non-ionic surfactant. Qualitatively very similar phase diagrams are obtained[14] with temperature playing the role of the surfactant-to-cosurfactant ratio or the ionic strength of the brine in multicomponent ionic surfactant mixtures.

This was the starting point of the present investigation. We wanted to find the most simple (*i.e.* binary) system showing dilute lamellar and L_3 phases. The advantage of binary water–non-ionic surfactant systems is that temperature is an easily controlled variable. Precise and reversible changes are useful when mapping out the phase diagram. Furthermore, the representation of a binary system in two dimensions is exact and the composition of coexisting phases can be obtained by the lever rule. The ambiguities in the interpretation of the results inherent in mixed-surfactant systems are avoided.

In the literature one finds examples of such binary systems with polyethylene glycol alkylethers as non-ionic surfactant.[15,16] At lower temperatures such systems display a phase behaviour, in common with the phase behaviour of ionic surfactants in aqueous solution. For several systems the phase sequence L_1–I_1–H_1–V_1–L_α appears with increasing surfactant concentration. (We here use the notation of Tiddy:[17] L_1, L_2 and L_3 denote isotropic liquid phases, I_1 and V_1 are micellar and bicontinuous cubic phases, respectively, H_1 is the normal hexagonal phase and L_α is the lamellar phase.) On the other hand, a very different phase behaviour occurs at higher temperatures where dilute L_3 and lamellar phases, and liquid–liquid coexistence regions, are observed. However, the lamellar phases in the quoted binary systems appeared to be much less stable with respect to dilution than in corresponding multicomponent mixtures. Therefore, reinvestigating the binary water–$C_{12}E_5$ system, we were surprised to find the L_3 and lamellar phases to swell to a much higher water content than has been previously reported.[16] The most striking observation was the swelling of the lamellar phase to almost 99 wt % water. While focusing on these two phases, we followed the swelling of the L_α phase with small-angle neutron scattering (SANS) and static light scattering, and investigated the L_3 phase by SANS and electrical-conductivity measurements.

Experimental

Materials

$C_{12}E_5$ was obtained fron Nikko, Japan. The purity was quoted to be better than 99% as measured by gas

† Present address: Division of Physical Chemistry 1, Chemical Center, University of Lund, P.O. Box 124, S-22100 Lund, Sweden.

View Article Online

Published on 01 January 1990. Downloaded by Max Planck Institut fuer on 11/01/2017 11:20:10.

chromatography. Water was doubly quartz distilled. Upon standing, in particular if in contact with air, the surfactant was found to degrade. Degradation results in a lowering of the critical temperature, T_c (cloud point). Since contact with air is difficult to avoid, especially when diluting with water, we performed the experiments within a few days of preparation of the samples.

The batch of $C_{12}E_5$ used for the phase-diagram determinations and in the static light-scattering experiments in the dilute lamellar phase was purified by a three-phase extraction technique,[18] which further removes oil and water-soluble contaminations from the surfactant. The purity of this batch is estimated to be better than 99.2% from gas chromatography.

Throughout this paper, except for in the presented phase diagrams, we have chosen to express the compositions in terms of volume fractions (Φ will denote the volume fraction of surfactant). When calculating these quantities we have used the following densities: H_2O, 0.998 g cm^{-3}; D_2O, 1.107 g cm^{-3}; $C_{12}E_5$, 0.9665 g cm^{-3}.

Phase Diagram

The data points shown on the experimental phase diagrams were determined in a thermostatted water bath with the samples contained in sealed test tubes. Phase-transition temperatures were determined by visual inspection in transmitted light, scattered light and between crossed polarizers. The temperature was controlled to a hundredth of a degree when necessary. For the low concentrations, *ca.* 1 wt % surfactant, macroscopic phase separation is a lengthy process and it was often several hours before the actual data points could be obtained by the lever rule.

Small Angle Neutron Scattering (SANS)

Neutron scattering experiments were performed on the beam lines PAXY and PAXE at LLB, Saclay, France. In order to enhance contrast, D_2O was used as solvent. Samples were prepared in cells which allow for orientation of lamellar liquid-crystalline phases. A cell, illustrated in fig. 1, consists of a rectangular (5 × 10 mm) Hellma quartz cell in which 25 thin (200 μm) quartz plates are stacked, equally spaced. This gives a spacing of *ca.* 200 μm between adjacent quartz surfaces. The cells were filled at room temperature and then heated to the temperature of the lamellar phase and shaken, in order to ensure homogeneity. Homogeneous samples were left to stand and a well oriented sample was obtained within a few hours.

The L_3 phase was prepared by allowing this phase to form upon heating of a homogeneous lamellar phase. For the experiments on this phase, the incoherent background scattering was subtracted from the experimental curves. For one sample, measurement on an absolute scale was made using the incoherent scattering of H_2O,[19] with a correction for the scattering of the cell when empty.

During scattering experiments, the samples were placed in a home-made cell holder with thermostat, allowing a temperature stability of *ca.* ±0.2 °C. Scattering experiments were performed in the planar configuration, *i.e.* with the quartz plates oriented with their normal perpendicular to the beam (*cf.* fig. 1). Some additional experiments were performed with 2 mm thick quartz cells. In particular, such a cell was used to perform absolute scale measurements.

Static Light Scattering (SLS)

Light scattering studies in the dilute regime of the lamellar phase were performed on a UV spectrometer (UV 860,

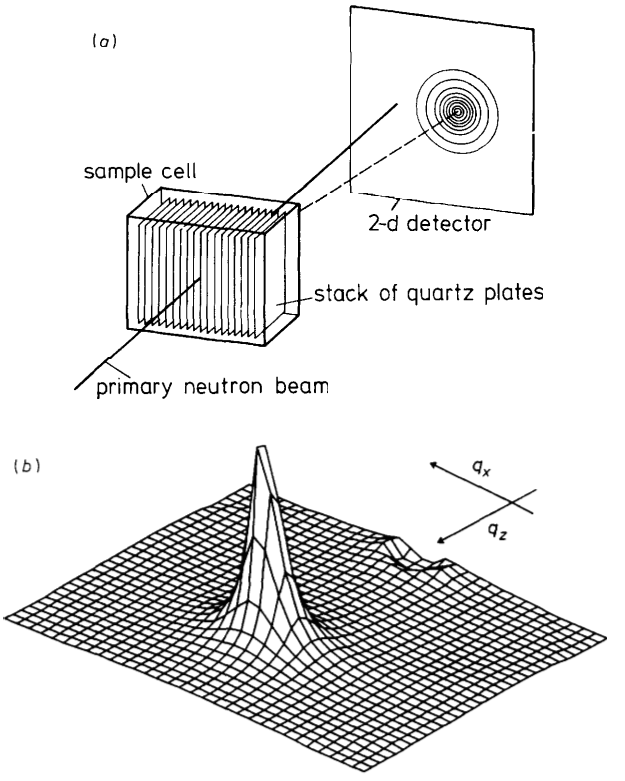

Fig. 1. (*a*) Schematic illustration of the cell and its configuration in the SANS experiments. Parallel quartz plates with a spacing of *ca.* 200 μm were sufficient to give a good orientation of the lamellar phase. (*b*) A 2-d SANS spectrum obtained in the L_α phase for $\Phi = 0.409$ at 57 °C.

Kontron) operating in transmission mode. Samples were contained in regular Beckman cuvettes. The reference beam was attenuated and a beam stop was placed behind the cuvette. The backward-scattered intensity was recorded at $\theta = 172 \pm 2°$ using a light guide (*cf.* fig. 2). The wave vector

$$q = \frac{4\pi n(\lambda)}{\lambda} \sin\left\{\frac{\theta}{2}\right\} \quad (1)$$

was calculated, assuming the refractive index, $n(\lambda)$, to be given by that of pure water and taking into account its wavelength dependence.[20]

Conductivity

Electrical conductivity was measured by a Wayne Kerr Autobalance Bridge B 960, operating at 1.5 kHz. The platinized cell had a cell constant of 0.78 cm^{-1}. The temperature control had an accuracy of ±0.01 °C at ambient temperatures and deteriorated to ±0.1 °C at 80 °C, still sufficient for the present purposes.

Phase Diagram

Upon studying the phase behaviour of the $C_{12}E_5$–water system we obtained the phase diagram shown in fig. 3. In fig. 3(*a*) the phase diagram in the interval 0–100 °C is given and in fig. 3(*b*) a selected temperature region, showing the swelling behaviour of the L_α and L_3 phases is drawn on a log scale. The phase diagram obtained in this study differs in some aspects from that previously reported.[16] The most striking observation is the swelling of the lamellar phase to almost 99% water around 58 °C. Fig. 3(*c*) shows a schematic phase diagram that, for reasons of clarity, is not drawn to scale.

View Article Online

Published on 01 January 1990. Downloaded by Max Planck Institut fuer on 11/01/2017 11:20:10.

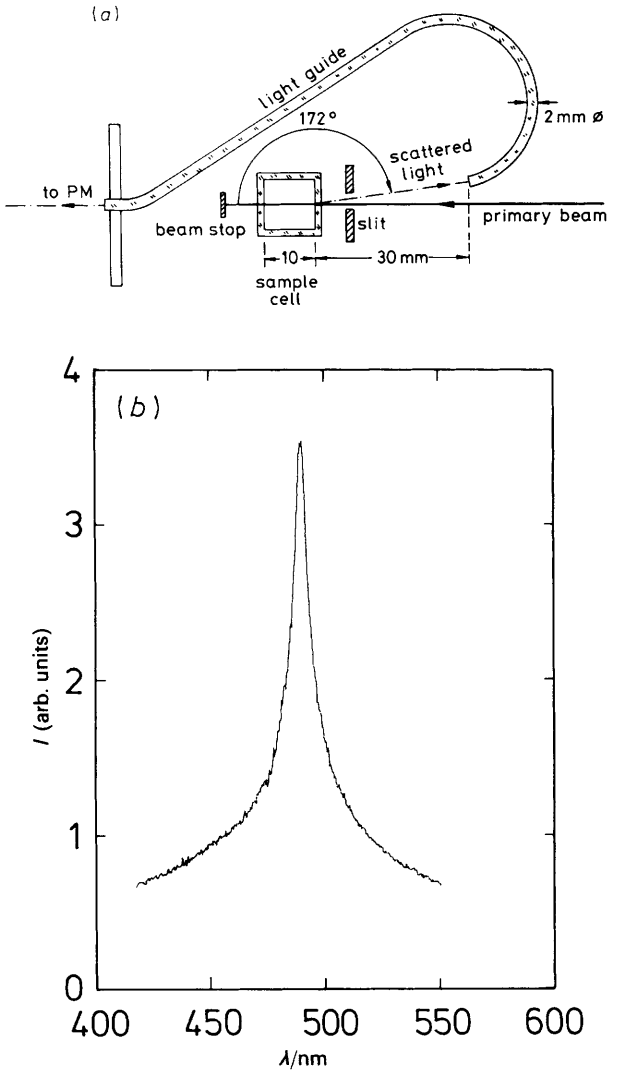

Fig. 2. (*a*) Schematic illustration of the experimental set up used in the light-scattering experiment. A UV spectrometer operating in transmission mode was used and the back-scattered intensity was recorded using a light guide connected to the PM tube. (*b*) A typical light-scattering spectrum recorded in the L_α phase for $\Phi = 0.0200$ at 57.6 °C.

At lower temperatures (*i.e.* below the cloud point) our phase diagram is in accordance with previous studies. The same phase sequence L_1–H_1–V_1–L_α–L_2(S) is observed and the respective melting points of the H_1 and V_1 phases obtained here are similar to those reported in ref. (16). However, at higher temperatures we have observed a significantly different phase behaviour. The lower critical temperature of the liquid–liquid coexistence region (cloud point) was in this study determined to be 31.9 °C. In ref. (16) a value of *ca.* 25 °C was reported. The $L_1' + L_1''$ coexistence we found to terminate at 54 °C and just above this temperature we found the L_α phase to swell to a very high water content, as is shown in fig. 3(*b*). Beyond the limit of swelling we observed the L_3 phase.

The phase behaviour around 54 °C, where the L_α phase dramatically swells to a very high dilution is rather complex within a narrow temperature region. For a sample of 5 wt % surfactant the evolution from $L_1' + L_1''$ coexistence to a homogeneous L_α phase takes place within *ca.* 0.1 °C. In a careful examination of this temperature region we observed experimentally a $L_3 + L_1''$ coexistence. This implies the existence of a three-phase line $L_1' + L_3 + L_1''$ separating these two biphasic regions. However, no other heterogeneous region could be detected between $L_3 + L_1''$ and L_α, as is expected from the phase rule. Several sequences for the following evolution from $L_3 + L_1''$ to L_α can be imagined. The simplest possible sequence following $L_3 + L_1''$ with increasing temperature, however, appears to be a second three-phase line $L_3 + L_1'' + L_\alpha$ followed by $L_3 + L_\alpha$ coexistence with increasing temperature. This sequence is outlined in the schematic phase diagram shown in fig. 3(*c*).

A similar complexity is found also around 81 °C, where the L_3 and L_α phases terminate. The maximum temperatures of the L_3 and L_α phases are quite similar. However, we found the L_3 phase to extend to a slightly higher temperature than L_α. Consequently, the L_α phase terminates at a three-phase line $L_3 + L_\alpha + L_2$ which appears at *ca.* 81 °C. The L_3 phase terminates at a three-phase line $L_1' + L_3 + L_2$ at a temperature of *ca.* 0.3 °C higher.

Our findings of a more narrow transition region around 54 °C than around 81 °C are consistent with a recent DSC study on the same system.[21] In this study only a single peak was resolved at 53.9 °C whereas two peaks were resolved around 80 °C.

Replacing H_2O with D_2O, as was done for the neutron scattering study, results in a lowering of the various transition temperatures. This isotopic effect is well known. No systematic study of the phase behaviour was performed with D_2O. However, we note that the L_α and L_3 phases were observed to swell even further with D_2O as solvent. A sample with $\Phi = 0.0082$ in D_2O showed a stable lamellar phase which should be compared with the maximum swelling of $\Phi = 0.012$ in H_2O.

The L_α phase appears relatively turbid when the concentration of surfactant is between 15 and 25 wt %. Moreover, macroscopic phase separation takes place rapidly if the temperature is too high or too low. For this reason it was not possible to prepare homogeneous samples in this concentration range in the cells for neutron scattering.

Lamellar Phase

Highly swollen lamellar phases are frequently found in ionic surfactant–alcohol systems.[22–24] Also some double-chained surfactants may swell considerably with water[25] or brine.[26] Highly swollen lamellar phases are also found in some alkenylsuccinic acid–water systems.[27] The observations in some systems where the lamellar phase swells to repeat distances of the order of 1 μm while retaining smectic order[28] are extraordinary. A common feature of the dilute lamellar phases, with repeat distances of the order of the wavelength of light, is that they appear coloured, due to Bragg scattering, when illuminated with white light. Several observations of coloured lamellar phases have been reported.[27–29]

In the present binary system, with non-ionic surfactant, the lamellar phase swells to almost 99 wt % of water within a rather narrow temperature region. The question of whether the inter-bilayer repulsion, leading to this swelling, is due to traces of ionic impurities has been studied by adding NaCl to the lamellar phase. A sample with a surfactant concentration of $\Phi = 0.0171$, showing a green colour in backscattering (the repeat distance is *ca.* 2000 Å), continued to show colours upon addition of salt up to 1 mol dm^{-3} NaCl which was considered to be sufficient to screen any electrostatic interaction. At this salt concentration the Debye length is *ca.* 3 Å. It therefore seems reasonable that the swelling of this lamellar phase is due to steric interactions.

View Article Online

Published on 01 January 1990. Downloaded by Max Planck Institut fuer on 11/01/2017 11:20:10.

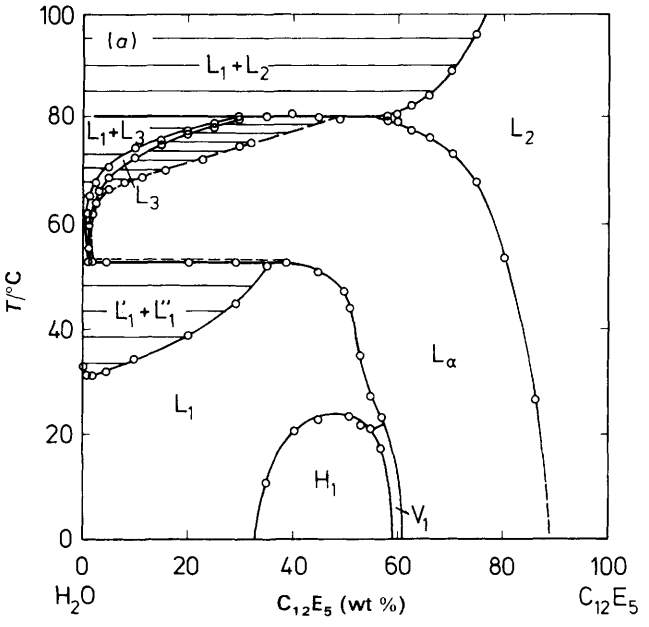

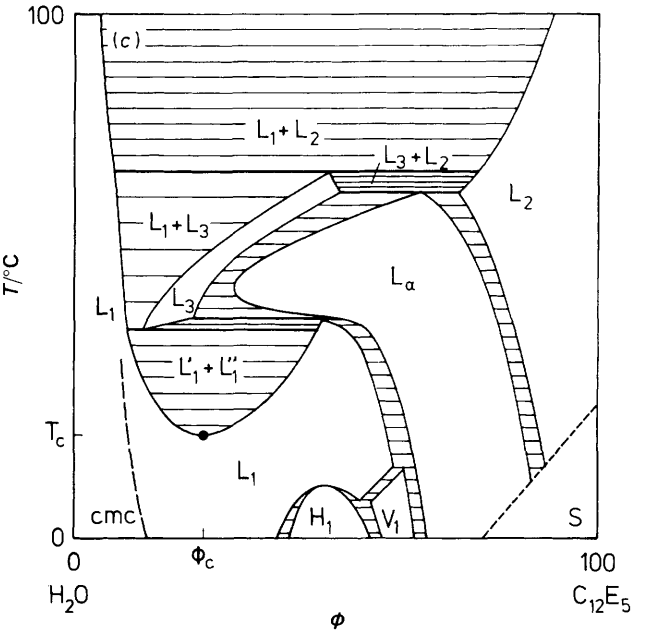

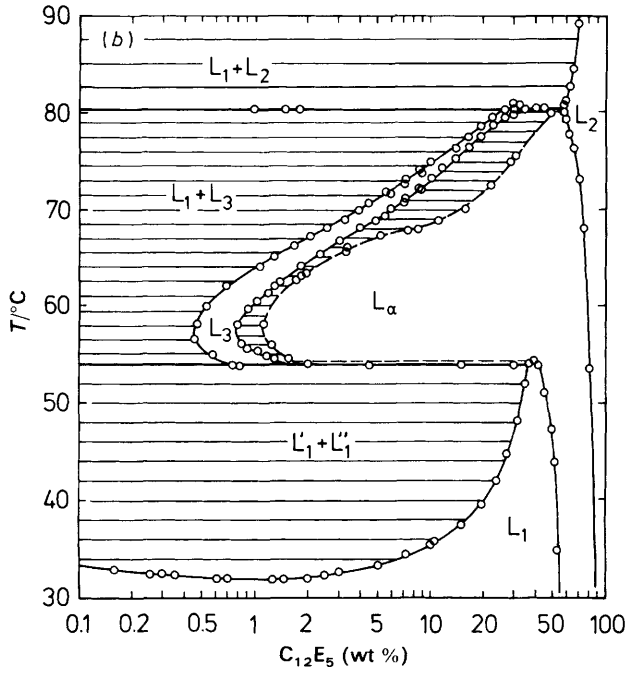

Fig. 3. Phase diagram of the water–$C_{12}E_5$ system. L_1, L_2 and L_3 denote isotropic liquid solutions, H_1 is a normal hexagonal phase, V_1 is a cubic liquid crystalline phase and L_α denotes a lamellar liquid crystalline phase. (*a*) The full diagram in the temperature range 0–100 °C. (*b*) A selected temperature range displaying in detail the swelling behaviour of the L_α and L_3 phases. Note that the compositions here are given on a logarithmic scale. (*c*) A schematic drawing of the full phase diagram. Note that this diagram is not drawn to scale.

Concentrated Regime—SANS

Neutron-scattering experiments have been performed on several samples in the concentration range $0.01 \leqslant \Phi \leqslant 0.4$, using D_2O as solvent. A particular feature of the experiments was that they were carried out on oriented samples. By studying planar-oriented samples with a two-dimensional (2-d) detector (*cf.* fig. 1), the scattering in the directions perpendicular, q_x, and parallel, q_z, to the symmetry axis are separated. A schematic illustration of the experimental set up and a 2-d spectrum are shown in fig. 1. As seen in fig. 1(*b*), a clear Bragg diffraction peak appears in the q_z direction. First-order Bragg reflections, that moved to low q with dilution, could be detected down to $\Phi = 0.032$.

For the more dilute samples ($\Phi \leqslant 0.1$) the spectra also showed significant anisotropic low-angle scattering, predominantly in the q_z direction, which became increasingly pronounced with dilution. Such low-angle scattering has been observed previously in other swollen lamellar phases.[30,31] It arises from concentration fluctuations normal to the bilayers[32] and is therefore a sign of thermal undulations.

The temperature dependence of the scattering spectrum was investigated for two samples, $\Phi = 0.103$ and 0.409, respectively, within the stability range of each composition. The peak positions remained constant as the temperature was varied and no change in small-angle scattering could be observed.

The phase transition L_α to L_3 was studied for one sample, $\Phi = 0.103$, by stepwise heating the sample from the L_α phase and recording the scattering spectrum. At the phase transition a diffuse isotropic (appear as circular on the 2-d detector) scattering peak was seen to coexist with, and grow at the expense of the anisotropic Bragg peak. Thus, indicating a clear, first-order transition.

Dilute Regime—Static Light Scattering

Light-scattering experiments were performed in the lamellar phase in the composition range $0.0126 \leqslant \Phi \leqslant 0.0303$. The detector angle was fixed and the spectrum of the scattered intensity was recorded as a function of the wavelength of the incident beam. The experimental set up is illustrated in fig. 2 together with a typical spectrum. Only a first-order peak was observed which was found to move to higher wavelength with dilution. As implied by the peak in the light-scattering spectrum, the dilute samples appear brilliantly coloured when irradiated with white light. A colour spectrum may be observed as a function of the angle to the light source. Note that the brilliance of the colours depends on the purity of the surfactant. A trace of oil made the colours disappear.

View Article Online

Published on 01 January 1990. Downloaded by Max Planck Institut fuer on 11/01/2017 11:20:10.

Evolution of the Bragg Peak Position with Dilution

Ideal one-dimensional swelling of a lamellar phase is described, assuming conservation of volume and a constant bilayer thickness, δ, by the relation

$$D = \frac{\delta}{\Phi} \tag{2}$$

where D is the repeat distance ($= 2\pi/q_1$, q_1 is the position of the first-order Bragg peak).

In fig. 4 we have plotted D, as obtained from SANS and static light scattering, as a function of $1/\Phi$. Note the large span in D, from 80 Å, for the most concentrated sample, to over 3000 Å, at very high dilution. The straight line represents a least-squares fit of eqn (2) to the data and corresponds to a one-dimensional swelling with a constant $\delta = 37.5$ Å. A closer inspection of the data in fig. 4 reveals a small systematic deviation from the simple relation of eqn (2). This is more evident for the light-scattering data which have a higher accuracy (±0.1–0.2%) than the SANS data (±5–10%). We will proceed to discuss possible deviations from eqn (2) on the basis of light-scattering data alone.

Remaining at the level of eqn (2), the most simple explanation that comes to mind about the observed deviation is to invoke a Φ dependence in the bilayer thickness. However, such a dependence is first of all expected to be negligible, considering the range of dilution ($0.0126 \leqslant \Phi \leqslant 0.0303$). Secondly, a decrease in δ, associated with an increase in headgroup area, is expected with dilution. Note also that the concentration of monomers is expected to be negligible. The critical micelle concentration (c.m.c.) is very low for long-chain non-ionic surfactants and $\Phi_{c.m.c.}$ is here estimated to be 3×10^{-5}, which is *ca.* 0.2% of Φ for the most dilute sample.

An alternative is to invoke defects. The two most commonly discussed types of defect are edge and screw dislocations. An example of the former type is simply a hole in a bilayer. Such defects, with radii larger than δ, will lead to an increase in the effective bilayer area in the system, and thus to a smaller D than is obtained from eqn (2) for a given composition. Screw dislocations, on the other hand, will, for small Φ, lead to a smaller effective area and hence to larger D. Consequently, the deviation observed in fig. 4 could, in principle, be explained by a decrease of the number of holes through the bilayers or, alternatively, by an increase in the number of screw dislocations upon dilution (or, of course, by a suitable linear combination of the two), given that such defects are present.

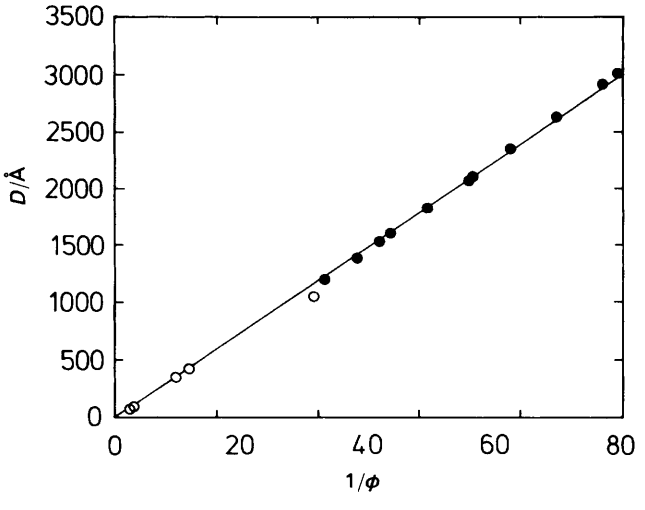

Fig. 4. The calculated repeat distance, D, plotted as a function of $1/\Phi$; (●) light scattering and (○) SANS data. (———) Least-squares fit of eqn (2) to the data, corresponding to $\delta = 37.5$ Å. Note the systematic deviation of the light-scattering data from eqn (2).

Finally, we may consider surfactant bilayers that are flexible and, owing to thermally induced undulations, are flat only on average. In this case, D will be larger than is given by eqn (2). The deviation will depend on the flexibility of the bilayer and on interbilayer interactions, and may be described by

$$D = \left\langle \frac{dA_{xy}}{dA_s} \right\rangle^{-1} \frac{\delta}{\Phi}. \tag{3}$$

The correction term $\langle dA_{xy}/dA_s \rangle \leqslant 1$ is the fraction of the total bilayer area that can be projected on the (x, y) plane perpendicular to the symmetry axis of the phase (the optical axis). Irrespective of the type of interbilayer repulsion (electrostatic or steric) $\langle dA_{xy}/dA_s \rangle$ is expected to decrease with dilution, owing to a decrease of the interaction, thus resulting in a deviation from eqn (2) in the same direction as observed.

When steric interactions dominate the repulsion we can estimate the area correction by starting from a free membrane for which a first-order correction to the projected area, owing to thermal undulations, has been derived[33]

$$\left\langle \frac{dA_{xy}}{dA_s} \right\rangle^{-1} = 1 + \frac{k_B T}{4\pi\kappa_0} \ln\left(\frac{q_{max}}{q_{min}}\right) \tag{4}$$

where q_{max} and q_{min} are UV and IR cut-offs, respectively, of the undulation modes and κ_0 is the bare rigidity constant. Eqn (4) may also serve as an estimate of the area correction in a stack of membranes by identifying the IR cut-off, $q_{min} = 2\pi/\xi$, where ξ is a length below which the bilayers appear to be free. This length has been estimated for the case of stacked, on average parallel, membranes a mean distance $\langle D \rangle$ apart[34,35]

$$\xi = c\langle D \rangle \left(\frac{\kappa_0}{k_B T}\right)^{1/2}. \tag{5}$$

Here, c is a numerical constant of the order of unity.[34,35] Taking the UV cut-off in eqn (4) to be $2\pi/\delta$ and using the approximation $\delta/\langle D \rangle = \Phi$ (corresponding to a zero-order correction within a first-order term) we may write

$$D = \frac{\delta}{\Phi}\left\{1 - \frac{k_B T}{4\pi\kappa_0} \ln\left[c^{-1}\left(\frac{\kappa_0}{k_B T}\right)^{-1/2}\Phi\right]\right\}$$
$$\approx \frac{\delta}{\Phi}\left(1 - \frac{k_B T}{4\pi\kappa_0} \ln \Phi\right) \tag{6}$$

where we assume $c \approx 1$ and $\kappa_0 \approx k_B T$. Thus, if steric interactions are important, we expect a logarithmic correction to the observed repeat distance.

In fig. 5 we have plotted $D\Phi$ as a function of $-\ln \Phi$. The data appear to fall on a straight line with a finite slope. Note that a horizontal line is expected from eqn (2). The full line in fig. 4 is a least-squares fit to the data and corresponds to $\delta = 30$ Å and $\kappa_0 = 1.3\ k_B T$. Thus, we find κ_0 to be of the order of $k_B T$, as expected if steric interaction stabilizes the lamellar phase at high dilution.

We note that this is the first time that an area correction may be quantitatively assigned to the swelling behaviour of a lamellar phase. The fact that we are dealing with a binary system (where we believe we can control the bilayer volume fraction) enables us to quantify a deviation from ideal one-dimensional swelling. However, we note also that the effect is very small and may, in principle, be due to defects if their

View Article Online

Published on 01 January 1990. Downloaded by Max Planck Institut fuer on 11/01/2017 11:20:10.

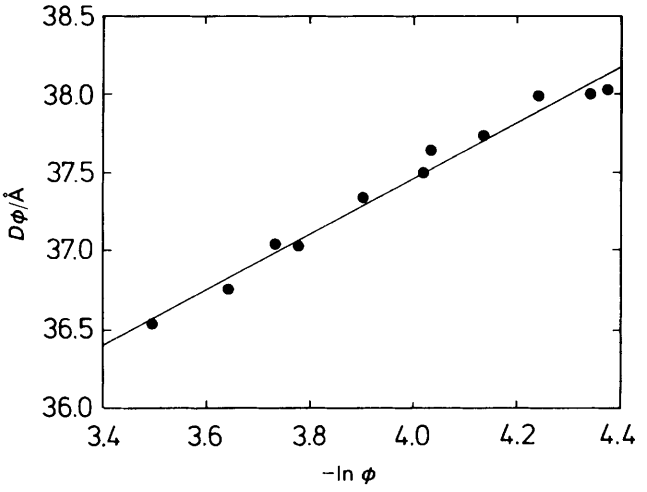

Fig. 5. $D\Phi$ plotted as a function of $-\ln \Phi$ for the light-scattering data. (———) Least-squares fit of eqn (6) to the data (see text). Note that a horizontal line is expected for ideal one-dimensional swelling.

concentration (counted as the fraction of the total surfactant concentration in defective regions) varies with dilution in certain particular ways. Moreover, the application of eqn (1) to the evaluation of the scattering vector may not be strictly valid in the case of Bragg scattering when the repeating distance in the medium is of the order of the wavelength of the light. On the other hand, if steric interactions are indeed effective, an effective area correction should be expected.

L_3 Phase

The appearance of an L_3 phase is a rather general property of surfactant systems and may be found in systems rich in water[14–16,22,23,36] as well as rich in oil,[22,36] most often adjacent to a swollen lamellar phase. This phase may join up continuously with other liquid phases and its significance has therefore not always been recognized, for example the narrow tongue extending from the L_2 phase towards the water corner observed in some studies of water–fatty acid–soap systems.[37,38] Its significance was probably first recognized from the observation of a second dilute isotropic liquid phase at higher temperatures, above the clouding temperature, for the water–$C_{12}E_5$ system[39] and of a narrow isotropic liquid region in the AOT–water–NaCl system.[26] The L_3 phase has, among other names, been termed 'anomalous',[15] owing to its particular macroscopic appearance. It may show strong opalescence and flow birefringence, properties which become increasingly pronounced with dilution.

The microstructure of this liquid phase and its stability relative to competing phases have recently received increasing attention.[30,40,41] From self-diffusion measurements the L_3 phase was first proposed to consist of disc micelles,[42,43] where the observed rapid surfactant diffusion[42] was ascribed to a rapid fusion and fission of micelles. It is now generally agreed that the structure is best described in terms of a 3-d continuous bilayer structure where a surfactant bilayer of highly connected topology forms a dividing surface separating two solvent domains.[30,40,41] Such a structure is compatible with recent small-angle X-ray and neutron-scattering studies, performed on aqueous and oil-rich solutions containing ionic surfactant, cosurfactant and salt.[30,44] It also explains the rapid surfactant diffusion[42] and receives further support from the high electrical conductivity observed in an oil-rich L_3 phase of a quinary system.[44]

In the present system, we have performed SANS and electrical conductivity measurements. Our results are in close agreement with and may, in part, serve as a generalization of previous findings. However, as will become evident, there are some properties which are more clearly observed in this binary system, belonging to the class of the most simple possible surfactant systems exhibiting an L_3 phase.

Conductivity

The electrical conductivity was measured in the L_3 phase after replacing water with a dilute aqueous solution of 0.1 wt % NaCl. Replacing water with brine had only a minor influence on the phase borders of the L_3 phase. The conductivity relative to pure brine is lower in the L_3 phase than in the L_1 phase at lower temperatures. This is clearly demonstrated in fig. 6 which shows a temperature scan of the specific conductivity, σ, for a sample with $\Phi = 0.113$ together with the temperature dependence of the conductivity of pure brine ($\Phi = 0$), σ_0. The curve in fig. 6 was measured by decreasing the temperature in steps of 0.3 °C, allowing 2 min for temperature equilibration. The solution was stirred continuously. We observed that increasing or decreasing the temperature yields practically the same curve.

The reduction of the specific conductivity when surfactant is added to brine is due to the trivial decrease of the brine volume fraction (addition of insulating units in the form of surfactant aggregates) and to the structural obstruction, caused by these aggregates, on the flow of ions in the medium. Thus, the reduced conductivity, σ', given by

$$\sigma' = \frac{\sigma}{\sigma_0(1 - \Phi)} \tag{8}$$

is expected to be sensitive, through obstruction effects, to the local microstructure in the solution. That this is at least qualitatively true, is clearly demonstrated by comparing the relative conductivity in the L_1 and L_3 phases (see fig. 6).

In fig. 7 we have plotted the reduced conductivity, σ', as a function of Φ. Here each sample was equilibrated in the middle of the temperature stability range. The conductivity was measured 1 min after turning of the stirrer. Throughout

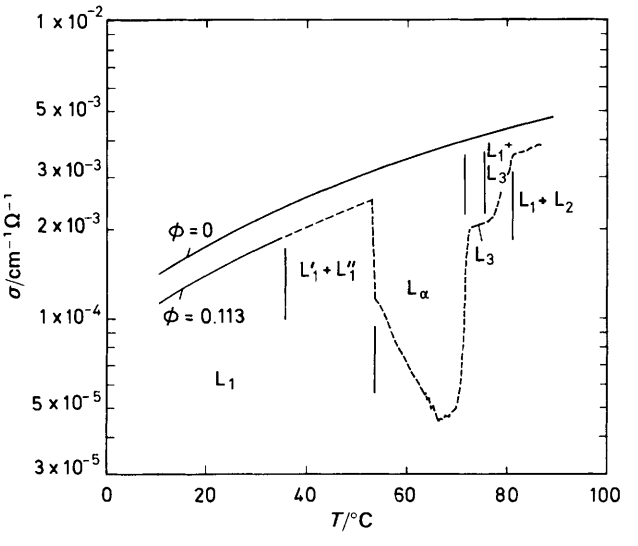

Fig. 6. A temperature scan of the specific conductivity, σ, for a water–$C_{12}E_5$ sample with $\Phi = 0.113$. The solvent is a 0.1 wt % aqueous solution of NaCl. The temperature dependence of the conductivity of pure brine ($\Phi = 0$) is also shown in the figure. Note the difference in conductivity relative to pure brine between the L_1 and L_3 phases.

View Article Online

Published on 01 January 1990. Downloaded by Max Planck Institut fuer on 11/01/2017 11:20:10.

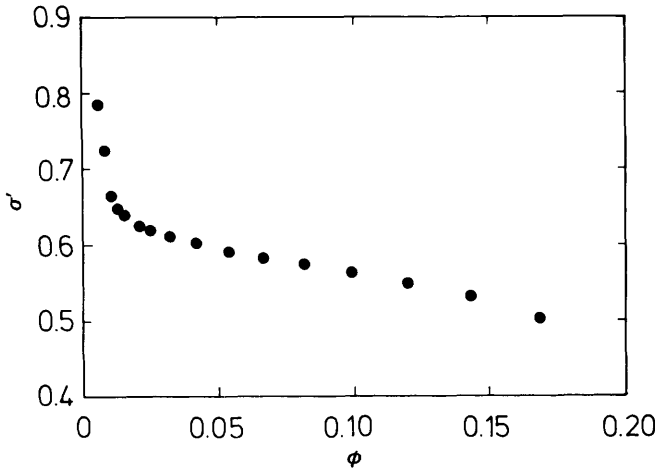

Fig. 7. A plot of the reduced conductivity, σ', defined by eqn (8), as a function of Φ in the L_3 phase. The temperature corresponds for each composition to approximately the middle of its stability range.

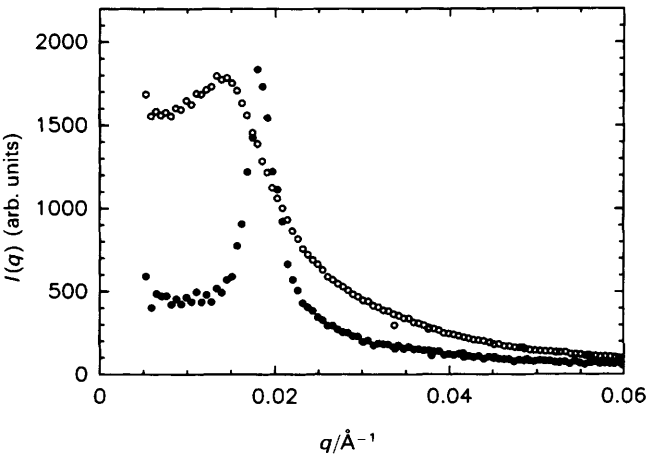

Fig. 8. SANS spectra recorded in the L_3 phase (○) and in the L_α phase (●), respectively, for $\Phi = 0.103$. The ratio between the two peak positions is *ca.* 1.2.

the L_3 phase, σ' is slightly reduced from unity (less than a factor of two). Two separate regimes of this dilution curve can be distinguished. In a concentrated regime, above $\Phi \approx 0.02$, we observe a moderate increase of σ' upon dilution. On the other hand, we observe a steep increase in σ' at dilutions beyond $\Phi \approx 0.02$.

The absolute values (slightly lower than 2/3) and the moderate slope of σ' observed for $\Phi > 0.02$ are both consistent with present concepts of structure involving a 3-d continuous bilayer structure.[45] In such a structure, the area-averaged mean curvature of the bilayer midplane vanishes by symmetry. However, the area-averaged mean curvature of the polar–apolar interface (surfactant headgroup region), $\langle H \rangle$, is towards the solvent[41] and varies with composition approximately as[41]

$$\Phi^2 \approx -1.1\delta\langle H \rangle \qquad (9)$$

[$\delta = 2L$ in ref. (41)]. Note that curvature towards brine is counted as negative. The slope in σ' may be qualitatively understood by considering that the flow of ions is obstructed by a surface that curves more and more towards brine when the surfactant concentration is increased. The geometrically disordered structure of the L_3 phase is topologically related to bilayer continuous cubic phases and similar transport properties are expected. The transport properties of some cubic phases have recently been calculated[45] and were found to be weakly topology dependent. Quantitatively, our data for $\Phi > 0.02$ are comparable to what is expected for a bilayer continuous cubic phase.

An interesting observation is the relatively steep increase in σ' with dilution below $\Phi \approx 0.02$. In this dilute regime we also observed a strong temperature dependence in the conductivity (σ' increases when the temperature is decreased) in contrast to the more concentrated regime where the conductivity was found to be insensitive to temperature. The increase of σ' above 2/3 indicates that the surfactant bilayer, close to the dilution limit, gradually breaks up into smaller fragments. The exact nature of these fragments (micelles, vesicles or fragments of bilayers with a topology similar to the structure at higher concentration) cannot be deduced from conductivity data alone.

SANS

Neutron-scattering experiments have been performed at various concentrations between $\Phi = 0.01$ and 0.1. Measurements at higher concentrations were not possible owing to the narrow stability range of the L_3 phase. A correlation peak could be detected only for the most concentrated sample.

The spectrum from this sample is shown in fig. 8. For comparison, a spectrum from the L_α phase, at a slightly lower temperature, is also shown. The position of the maximum of the diffuse liquid peak, q_{max}, appears at low q relative to the first-order Bragg peak, q_1, in the L_α phase. The ratio q_1/q_{max} is here about 1.2. The structure factor of complex liquids, such as the L_3 phase and the related bicontinuous microemulsions, has been approached by several authors[46–49] from different starting points. One of these[49] predicts $q_1/q_{max} = 1.5$ from a cubic tesselation model. The value is related to the number of nearest neighbours in lattice models, and a Voronoi tesselation yields 1.46. Values close to 1.5 have also been extracted from the dilution properties of q_{max} in L_3 phases of the more complex ionic surfactant–cosurfactant systems.[30,44] The present observation is restricted to a single composition, however, a similar value may be observed in related bicontinuous ternary microemulsion systems with non-ionic surfactant.[50] We postpone a further discussion of this topic, but note that systems with non-ionic surfactants appear to be the most suitable for experimental studies of the structure factor in dilute L_3 phases and microemulsions.

In order to investigate the asymptotic scattering at $q > q_{max}$ it is convenient to present the scattering curve on a log–log scale. Fig. 9 shows the scattering, in absolute units, from a sample with $\Phi = 0.0841$ in the L_3 phase. A large part of the scattering curve in the asymptotic range can be accounted for by the single-particle, isotropically averaged form-factor of an infinite lamella.[51] In the case of a $C_{12}E_5$ bilayer, we expect the scattering length-density profile to be somewhat thinner than the surfactant mass-density profile since the ethylene oxide headgroups mix with D_2O. Modelling, for simplicity, these two profiles as square wells, characterized by thicknesses δ' and δ [note that this is equivalent to δ in eqn (2)], respectively, we obtain, starting from the single-particle expression,[51] the normalized scattering intensity, $I(q)$

$$I(q) = \frac{\Phi}{\delta} 2\pi\delta'^2(\Delta\rho)^2 q^{-2}\left[\frac{\sin(q\delta'/2)}{q\delta'/2}\right]^2. \qquad (10)$$

Here the factor (Φ/δ) arises from the incoherent addition of the intensities scattered by an assembly of uncorrelated infinite lamellae and $\Delta\rho$ is the difference in scattering length density between solvent and lamellae. A fit of eqn (10) to the

View Article Online

Published on 01 January 1990. Downloaded by Max Planck Institut fuer on 11/01/2017 11:20:10.

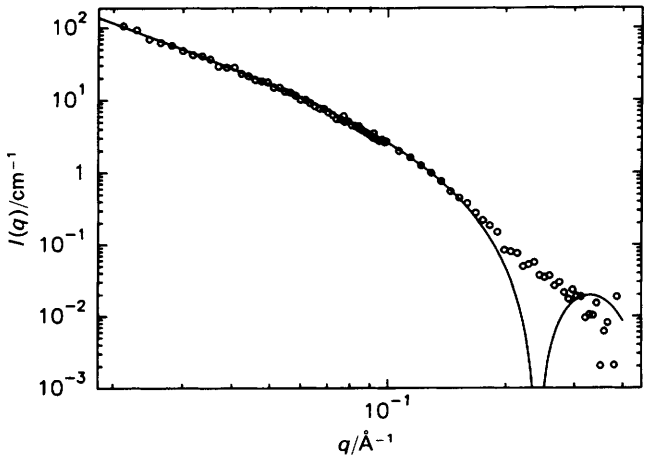

Fig. 9. SANS spectrum recorded in the L_3 phase for $\Phi = 0.0841$, plotted on a log–log scale. The intensity is in absolute units (cm^{-1}). The solid line corresponds to the form-factor of an infinite lamellae [eqn (10)] with $\Delta\rho = 5.7 \times 10^{10}$ cm^{-2} and $\delta' = 26$ Å.

data is shown in fig. 9 as a solid line. With $\Phi = 0.084$ and the width of the mass-density profile taken from the study of the lamellar phase to be $\delta = 30$ Å, the fit yields $\delta' = 26$ Å and $\Delta\rho = 5.9 \times 10^{10}$ cm^{-2}. The width of the scattering length density profile is, as expected, smaller than δ. Its depth is close to, but slightly smaller than, the value 6.8×10^{10} cm^{-2}, corresponding to the contrast between D_2O and the surfactant hydrocarbon tails, which is consistent with the fact that the bilayers contain lower contrasted ethylene oxide groups.

At wavevectors larger than $2\pi/\delta'$, the assumed discontinuity in the scattering length-density profile introduces spurious oscillations, as implied by eqn (10). The absence of such oscillations in the experimental scattering curve could, in principle, be explained by invoking a polydispersity in the bilayer thickness, but is more likely to be related to a smoother profile of the scattering length density across the bilayer.

The scattering curves from different concentrations are very similar, indicating similar local structure. When normalizing the intensities with $1/\Phi$, as suggested by eqn (10), the scatterings from different concentrations fall practically on the same curve. This is demonstrated in fig. 10 where we have

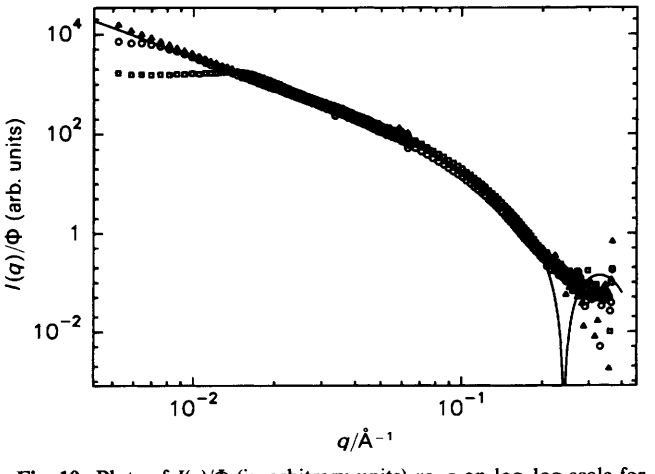

Fig. 10. Plots of $I(q)/\Phi$ (in arbitrary units) *vs.* q on log–log scale for three different compositions in the L_3 phase. The various compositions are $\Phi = 0.011$ (▲), $\Phi = 0.053$ (○) and $\Phi_s = 0.10$ (□). Note the similar asymptotic scattering, including the scaling of the scattered intensity as $1/\Phi$, for the different compositions.

plotted $I(q)/\Phi$ for three different concentrations in the L_3 phase.

To summarize, the scattering curves obtained in this study are very similar to those obtained in L_3 phases of quaternary and quinary systems[30,44] and are consistent with a local bilayer structure.

Conclusions

We have investigated the binary water–$C_{12}E_5$ system and shown that dilute lamellar and L_3 phases, previously observed only in more complex surfactant systems, may indeed be observed and investigated in simple binary mixtures. Our results from investigating the present system confirm several results obtained in more complex systems. Furthermore, the simplicity of the present system allows us to observe: (i) an area correction to the repeat distance in the swelling of the lamellar phase, (ii) a Φ dependence of the electrical conductivity in the L_3 phase and (iii) a break up of the structure in the L_3 phase at very high dilution.

We are indebted to Prof. M. Kahlweit for his support. We also thank T. Lieu for the help with the phase-diagram determination, J. Winkler for the conductivity measurements, Y. Hendrikx and J. Charvolin for providing us with the cells for the SANS measurements and L. Auvray and A. Brulet for helpful assistance at L.L.B. D. M. Anderson and H. Wennerström are kindly acknowledged for communicating a preprint prior to publication. U.O. thanks the Swedish Board of Technical Development (STU) for financial support during his stay at C.R.P.P. The present work has been performed under partial support by the European Community.

References

1 P. Ekwall, L. Mandell and K. Fontell, *Mol. Cryst. Liq. Cryst.*, 1969, **8**, 157.
2 *Physics of Amphiphilic Layers*, Springer Proceedings in Physics, vol. 21, ed. D. Langevin, J. Meunier and N. Boccara (Springer-Verlag, Heidelberg, 1987).
3 D. Roux, in *Random Fluctuations and Pattern Growth: Experiments and Models*, ed. H. E. Stanley and N. Ostrowsky (Kluwer Academic Publishers, The Netherlands, 1988), p. 246.
4 W. Helfrich, *Phys. Lett. A*, 1973, **43**, 409.
5 W. Helfrich, *Naturforsch.*, 1978, **33a**, 305.
6 C. R. Safinya, D. Roux, G. S. Smith, S. K. Sinha, P. Dimon, N. A. Clark and A. M. Bellocq, *Phys. Rev. Lett.*, 1986, **57**, 2718.
7 D. Roux and C. R. Safinya, *J. Phys. France*, 1988, **49**, 307.
8 F. Nallet, D. Roux and J. Prost, *Phys. Rev. Lett.*, 1989, **62**, 276.
9 F. Nallet, D. Roux and J. Prost, *J. Phys. France*, 1989, **50**, 3147.
10 C. R. Safinya, E. B. Sirota, D. Roux and G. S. Smith, *Phys. Rev. Lett.*, 1989, **62**, 1134.
11 M. Kahlweit, R. Strey, P. Firman, D. Haase, J. Jen and R. Schomäcker, *Langmuir*, 1988, **4**, 499.
12 M. Kahlweit, R. Strey, R. Schomäcker and D. Haase, *Langmuir*, 1989, **5**, 305.
13 M. Kahlweit, R. Strey, D. Haase, H. Kunieda, T. Schmeling, B. Faulhaber, M. Borkovec, H-F. Eicke, G. Busse, F. Eggers, Th. Funck, H. Richmann, L. Magid, O. Söderman, P. Stilbs, J. Winkler, A. Dittrich and W. Jahn, *J. Colloid Interface Sci.*, 1987, **118**, 436.
14 U. Olsson, P. Ström, O. Söderman and H. Wennerström, *J. Phys. Chem.*, 1989, **93**, 4572.
15 J. C. Lang and R. D. Morgan, *J. Chem. Phys.*, 1980, **73**, 5849.
16 D. J. Mitchell, G. J. T. Tiddy, L. Waring, T. Bostock, M. P. McDonald, *J. Chem. Soc., Faraday Trans. 1*, 1983, **79**, 975.
17 G. J. T. Tiddy, *Phys. Rep.*, 1980, **57**, 1.
18 K-V. Schubert, *Diplomarbeit* (University of Göttingen, 1989) and to be published.
19 B. Jacrot, *Rep. Prog. Phys.*, 1976, **39**, 911.
20 H. Eisenberg, *J. Chem. Phys.*, 1965, **43**, 3887.
21 B. Andersson and G. Olofsson, *Colloid Polym. Sci.*, 1987, **265**, 318.

View Article Online

22 A. M. Bellocq and D. Roux, in *Microemulsions: Structure and Dynamics*, ed. S. Friberg and P. Bothorel (CRC Press, Boca Baton, 1987), p. 33.
23 W. J. Benton and C. A. Miller, *J. Phys. Chem.*, 1983, **87**, 4981.
24 F. C. Larche, J. Appell, G. Porte, P. Bassereau and J. Marignan, *Phys. Rev. Lett.*, 1986, **56**, 1700.
25 G. G. Warr, R. Sen, D. F. Evans and J. E. Trend, *J. Phys. Chem.*, 1988, **92**, 774.
26 K. Fontell, in *Colloidal Dispersions and Micellar Behavior*, ACS Symposium Series 9 (American Chemical Society, Washington DC, 1975), p. 270.
27 N. Satoh and K. Tsujii, *J. Phys. Chem.*, 1987, **91**, 6629.
28 J. Appell, P. Bassereau, J. Marignan and G. Porte, *Colloid Polym. Sci.*, 1989, **267**, 600.
29 T. Imae, M. Sasaki and S. Ikeda, *J. Colloid Interface Sci.*, 1989, **131**, 601.
30 G. Porte, J. Marignan, P. Bassereau and R. May, *J. Phys. France*, 1988, **49**, 511.
31 F. Nallet and D. Roux, unpublished.
32 G. Porte, J. Marignan, P. Bassereau and R. May, *Europhys. Lett.*, 1988, **7**, 713.
33 W. Helfrich, *J. Phys. France*, 1985, **46**, 1263.
34 S. Leibler and R. Lipowsky, *Phys. Rev. B*, 1987, **35**, 7004.
35 L. Golubovic and T. C. Lubensky, *Phys. Rev. B*, 1989, **39**, 12110.
36 H. Kunieda and K. Shinoda, *J. Dispersion Sci. Technol.*, 1982, **3**, 233.
37 J. W. McBain and M. C. Field, *J. Am. Chem. Soc.*, 1935, **55**, 4776.
38 P. Ekwall and L. Mandell, *Kolloid Z.*, 1969, **233**, 938.
39 F. Harusawa, S. Nakamura and T. Mitsui, *Colloid Polym. Sci.*, 1974, **252**, 613.
40 M. E. Cates, D. Roux, D. Andelman, S. T. Millner and S. A. Safran, *Europhys. Lett.*, 1988, **5**, 733.
41 D. Anderson, H. Wennerström and U. Olsson, *J. Phys. Chem.*, 1989, **93**, 4243.
42 P-G. Nilsson and B. Lindman, *J. Phys. Chem.*, 1984, **88**, 4764.
43 C. A. Miller and O. Ghosh, *Langmuir*, 1986, **2**, 321.
44 D. Gazeau, A. M. Bellocq, D. Roux and T. Zemb, *Europhys. Lett.*, 1989, **9**, 447.
45 D. M. Anderson and H. Wennerström, *J. Phys. Chem.*, in press.
46 N. F. Berk, *Phys. Rev. Lett.*, 1987, **58**, 2718.
47 M. Teubner and R. Strey, *J. Chem. Phys.*, 1987, **87**, 3195.
48 T. N. Zemb, S. T. Hyde, P-J. Derian, I. Barnes and B. W. Ninham, *J. Phys. Chem.*, 1987, **91**, 3814.
49 S. T. Milner, S. A. Safran, D. Andelman, M. E. Cates and D. Roux, *J. Phys. France*, 1988, **49**, 1065.
50 F. Lichterfeld, T. Schmeling and R. Strey, *J. Phys. Chem.*, 1986, **90**, 5762.
51 O. Glatter and O. Kratky, *Small Angle X-Ray Scattering* (Academic Press, New York, 1982).

Paper 9/05287I; *Received* 12*th December*, 1989

Published on 01 January 1990. Downloaded by Max Planck Institut fuer on 11/01/2017 11:20:10.